Iowa State University

DETERMINATION OF THE AERODYNAMIC PERFORMANCE OF A LOW-SPEED AIRFOIL BASED ON PRESSURE DISTRIBUTION MEASUREMENTS LABORATORY

AER E 344 - Lab 05 - Determination of the Aerodynamic Performance of a Low-Speed Airfoil based on Pressure Distribution Measurements

Section 3 Group 3

Matthew Mehrtens
Jack Mendoza
Kyle Ostendorf
Gabriel Pederson
Lucas Tavares Vasconcellos
Drew Taylor

Professor

Hui Hu, PhD

College of Engineering

Aerospace Engineering

Aerodynamics and Propulsion Laboratory

Ames, March 2024

Abstract

Studying the aerodynamic characteristics of airfoils is a critical process in subscale testing. Using the low-speed wind tunnel at Iowa State University with several pressure transducers, we measured the pressure over a GA(W)-1 for various angles of attack. Based on our analysis and visualize of the data using a MATrix LABoratory (MATLAB) script, we found the stall angle was 12°. Additionally, we found that the stagnation point occurred at the tip of the airfoil for low angle of attack (AoA) and moved slightly to the right on the lower side of the airfoil for higher angles of attack. Our coefficient of pressure graphs also allowed us to identify when and to what degree the flow was separating on top of the airfoil when it underwent higher angles of attack.

Contents

List of Figures

List of Tables

Glossary

A'	Total axial component of the pressure force acting on the airfoil. *(p. 6)*
C_P	Dimensionless coefficient of pressure. *(p. iv, 9, 10, 12, 13, 15–17, 20–22)*
C_d	Dimensionless coefficient of drag. *(p. iii, iv, 5–7, 12, 13, 22)*
C_l	Dimensionless coefficient of lift. *(p. iii, iv, 5–7, 12, 13, 22)*
C_m	Dimensionless coefficient of moment. *(p. iii, iv, 5–7, 13, 22)*
D'	Drag force per unit span. *(p. 6)*
L'	Lift force per unit span. *(p. 6)*
M'_{LE}	Total moment force caused by the pressure forces acting on the airfoil. *(p. 6)*
N	Number of panels making up the airfoil surface. *(p. 4)*
N'	Total normal component of the pressure force acting on the airfoil. *(p. 6)*
Δx_i	Distance between two x-coordinates. *(p. 5)*
Δx_i	Distance between two y-coordinate. *(p. 5)*
α	Angle of attack of an airfoil. *(p. 6)*
$\delta A'_i$	Axial component of the pressure force acting on the ith panel. *(p. 5)*
$\delta M'_{LE,i}$	Aerodynamic moment on the ith panel caused by the pressure forces on the airfoil. *(p. 5)*
$\delta N'_i$	Normal component of the pressure force acting on the ith panel. *(p. 5)*
p_i	Pressure at the ith pressure tap. *(p. 5)*
$p_{i+1/2}$	Pressure at the ith panel on the airfoil. *(p. 5)*
x_i	x-coordinate for the ith pressure tap. *(p. 4, 5)*
y_i	y-coordinate for the ith pressure tap. *(p. 4, 5)*

Acronyms

AoA angle of attack. *(p. i, 4, 9, 10, 12, 15–17)*

MATLAB MATrix LABoratory. *(p. i, 6)*

1 Introduction

The Scanivalve DSA 3217, a 16-channel digital pressure transducer pictured in Figure A.7, calculates the differences in pressure between the input ports and the calibrated reference pressure. In this experiment, the ports of the pressure transducer are connected to pressure taps that line the surface of an airfoil (see Figure 2.2), numbered in the clockwise direction. The Scanivalve pressure transducer is also measuring the pressure at the inlet and outlet of the contraction section.

Using three Scanivalve pressure transducers in conjunction with the data acquisition software, we will measure the pressure around the airfoil (see Section B.1). After post-processing using the script in Section C.1, we will describe the results of the data in Chapter 3 and Chapter 4.

2 METHODOLOGY

2.1 Apparatus

An airfoil is positioned in the wind tunnel test chamber as seen in Figure 2.1. The airfoil contains pressure taps around its surface connected to three Scanivalve pressure transducers. Figure 2.2 shows the tubes connecting the airfoil pressure taps to the Scanivalve pressure transducers. A computer with data acquisition software collects measurements from the pressure transducers and stores the data in `.csv` files.

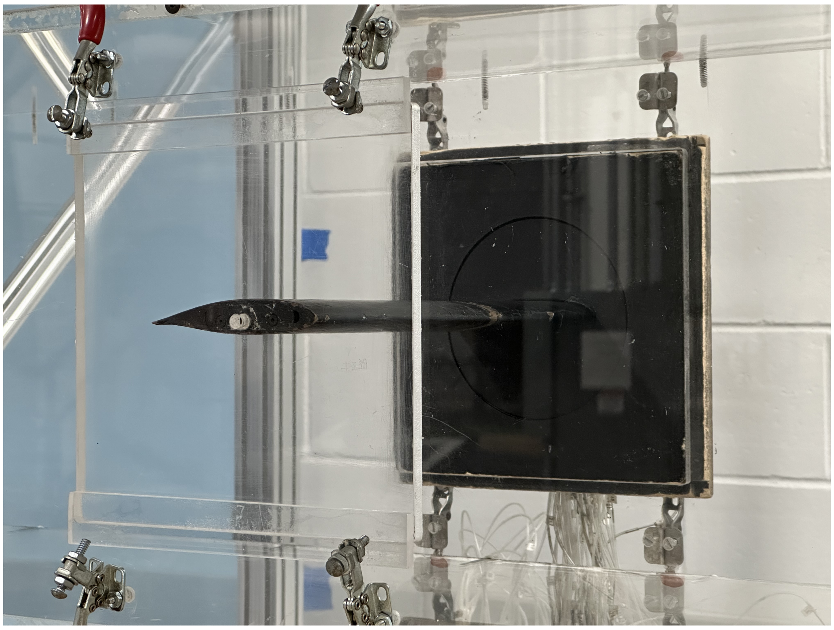

Figure 2.1: *Image of Airfoil in Test Section.*

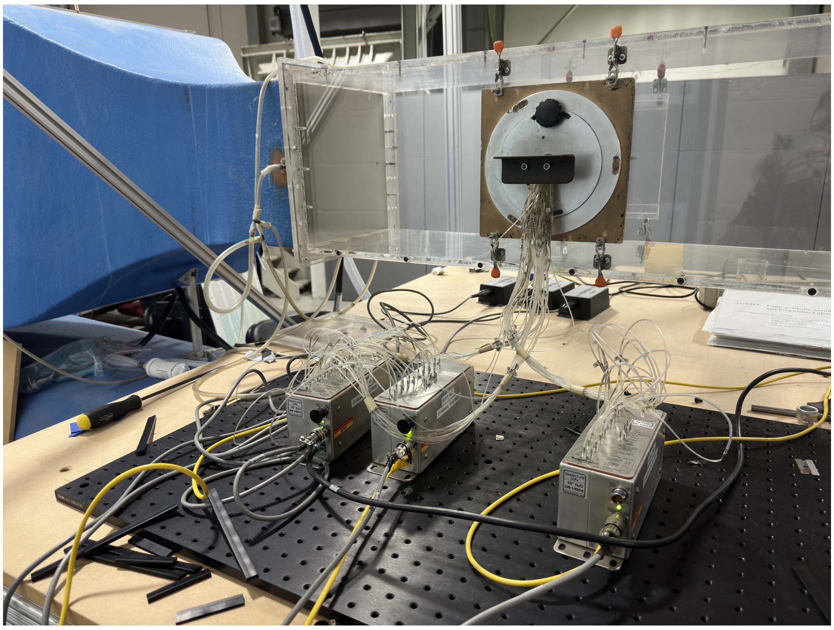

Figure 2.2: *Image of the Scanivalve tester next to the test section.*

2.2 Procedure

1. Determine the correct motor frequency to use for a wind tunnel velocity of 10 m/s to 15 m/s.
2. Verify the connections to the three Scanivalve pressure transducers.
3. Using the data acquisition software, calibrate the three Scanivalve pressure transducers.
4. Set the wind tunnel to 10 m/s to 15 m/s.
5. Set the AoA to $-4°$.
6. Using the data acquisition software, start a file, press the "Start" button, press the "Close File" button, and then change the AoA according to the lab manual.
7. Repeat step 6 for AoA $-4°$, $0°$, $4°$, $6°$, $8°$, $10°$, $12°$, $14°$ and $16°$.
8. Repeat step 6 and step 7 as many times as time allows.
9. Save the data to a flash drive for post-lab analysis.

2.3 Derivations

The surface of the airfoil can be broken into N panels. For a generic, ith panel, the panel boundaries come from the ith and $i+1$th taps at (x_i,y_i) and (x_{i+1}, y_{i+1}). This expression is valid for all the panels except the Nth panel, which is bounded by a fictitious $N+1$ tap that takes on the value of the first tap.

To determine the pressure acting on each panel of the airfoil—which is the average of the pressure between two pressure taps—we use

$$\begin{cases} p_{i+1/2} = \frac{1}{2}(p_i + p_{i+1}) \\ p_{N+1/2} = \frac{1}{2}(p_N + p_1) \end{cases} \tag{2.1}$$

where $p_{i+1/2}$ is the averaged pressure at the ith panel and p_i is the pressure measured at the ith pressure tap.

To find the lift, drag, and moment forces over the airfoil, we use trapezoidal integration. Before we can integrate, we must define

$$\begin{cases} \Delta x_i = x_{i+1} - x_i, \qquad \Delta y_i = y_{i+1} - y_i \\ \Delta x_N = x_1 - x_N, \qquad \Delta y_N = y_1 - y_N \end{cases} \tag{2.2}$$

where Δx_i and Δx_i are the distances between the ith pressure tap and the $i+1$th pressure tap in the x and y coordinate systems respectively and x_i and y_i is the location of the ith pressure tap in the x and y coordinate system. Figure 2.3 shows the generalized trapezoid used to integrate.

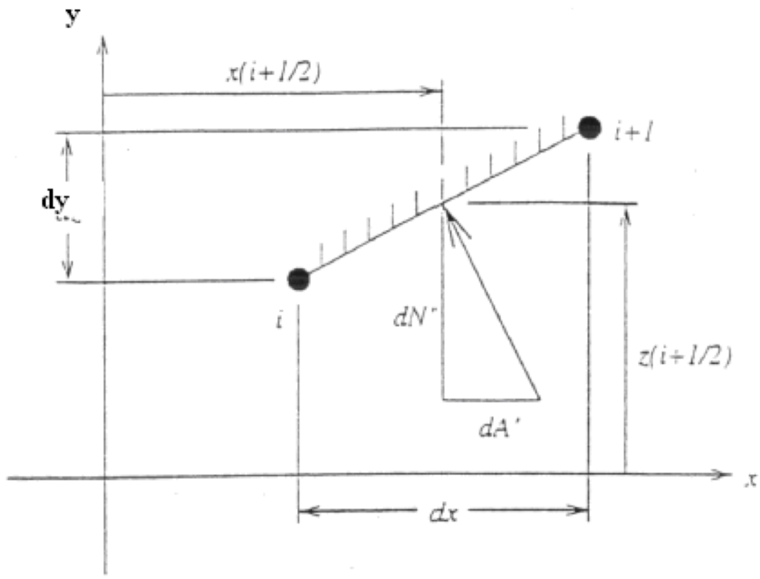

Figure 2.3: *A diagram of the trapezoidal integration used to calculate C_l, C_d, and C_m (Hu, 2024).*

Using Equation 2.1 and Equation 2.2, we can derive the following force per unit span components:

$$\delta N_i' = p_{i+1/2}\Delta x_i \tag{2.3}$$

$$\delta A_i' = -p_{i+1/2}\Delta y_i \tag{2.4}$$

$$\delta M_{LE,i}' = -\left(p_{i+1/2}\Delta x_i\right) x_{i+1/2} - \left(p_{i+1/2}\Delta y_i\right) y_{i+1/2} \tag{2.5}$$

where $\delta N_i'$ is the normal component of pressure on the ith panel, $\delta A_i'$ is the axial component of pressure on the ith panel, $\delta M_{LE,i}'$ is the aerodynamic moment force on the ith panel, and $x_{i+1/2}$ and $y_{i+1/2}$ are defined as

$$x_{i+1/2} = \frac{1}{2}(x_i + x_{i+1}) \tag{2.6}$$

$$y_{i+1/2} = \frac{1}{2}(y_i + y_{i+1}) \tag{2.7}$$

Once each component of the aerodynamic forces is calculated, we sum the component to find the total aerodynamic forces per unit span as shown blow:

$$N' = \sum_{i=1}^{N} \delta N'_i \tag{2.8}$$

$$A' = \sum_{i=1}^{N} \delta A'_i \tag{2.9}$$

$$M'_{LE} = \sum_{i=1}^{N} \delta M'_{LE,i} \tag{2.10}$$

where N' and A' are the sums of the pressure forces in the normal and axial directions respectively and M'_{LE} is the total moment caused by the pressure forces on the airfoil. We can use N' and A' to find the lift and drag forces per unit span, L' and D', respectively:

$$L' = N' \cos\alpha - A' \sin\alpha \tag{2.11}$$

$$D' = N' \sin\alpha + A' \cos\alpha \tag{2.12}$$

where α is the angle of attack.

To find the coefficients of lift, drag, and moment—C_l, C_d, and C_m, respectively—we must also calculate the dynamic pressure, $q = \frac{1}{2}\rho v^2$. Then, using the forces per unit span we derived above and dividing them by the dynamic pressure, we find

$$C_l = \frac{L'}{q} \tag{2.13}$$

$$C_d = \frac{D'}{q} \tag{2.14}$$

$$C_m = \frac{M'_{LE}}{q} \tag{2.15}$$

Finally, we wrote a MATrix LABoratory (MATLAB) script to visualize the data into graphs (see Section C.1).

3
Results

Figure 3.1, Figure 3.2, and Figure 3.3 show the coefficient of lift, drag, and moment—C_l, C_d, and C_m—at angles of attack of $-4°$ to $16°$. These were calculated using the formulas described in Section 2.3 and the script shown in Section C.1.

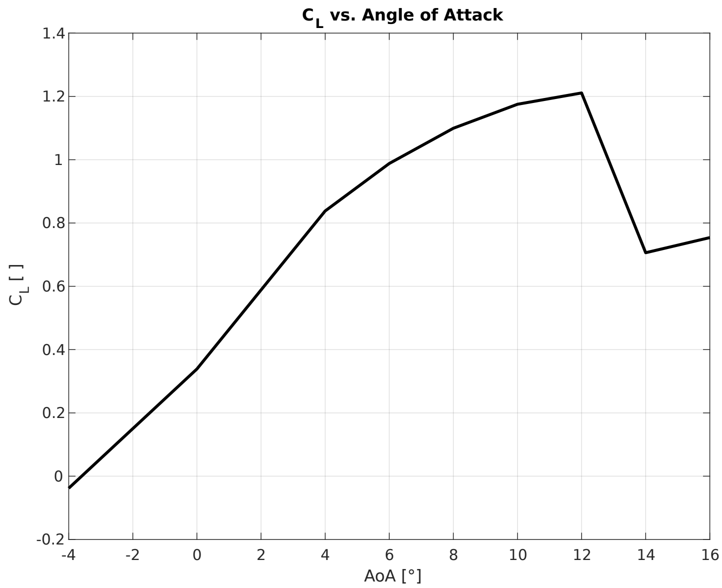

Figure 3.1: *Plot of the Coefficient of Lift vs. Angle of Attack.*

Figure 3.4, Figure 3.5, Figure 3.6, and Figure 3.7 show the coefficient of pressure along the upper and lower surfaces of the airfoil for the respective angle of attack. These were calculated using equations derived in Section 2.3 with the code shown in Section C.1.

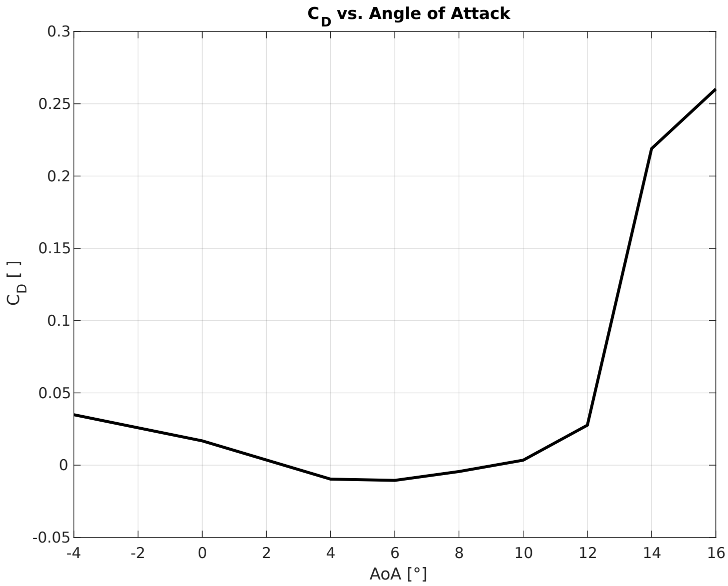

Figure 3.2: *Plot of the Coefficient of Drag vs. Angle of attack.*

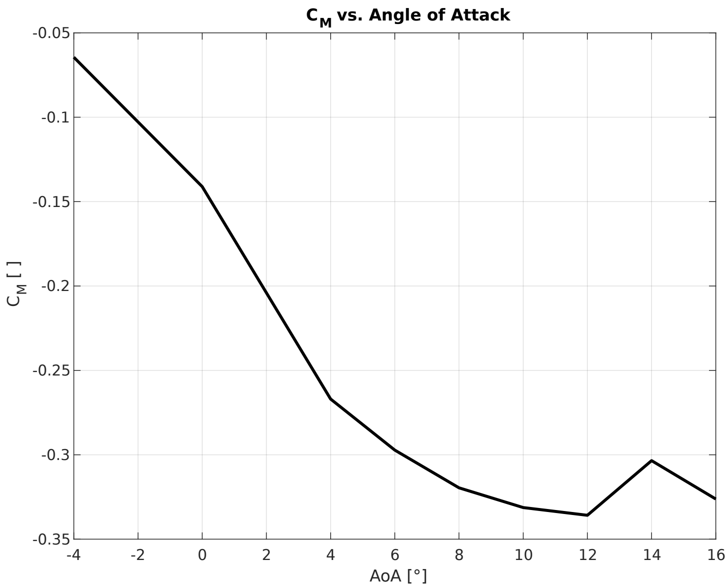

Figure 3.3: *Plot of the Moment Coefficient vs. Angle of attack.*

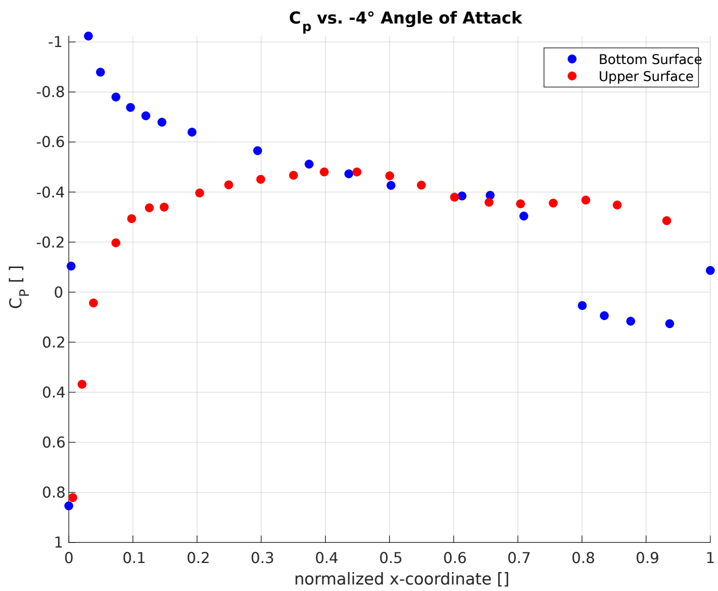

Figure 3.4: *Plot of the C_P in relationship to the normalized x component at an AoA of* $-4°$.

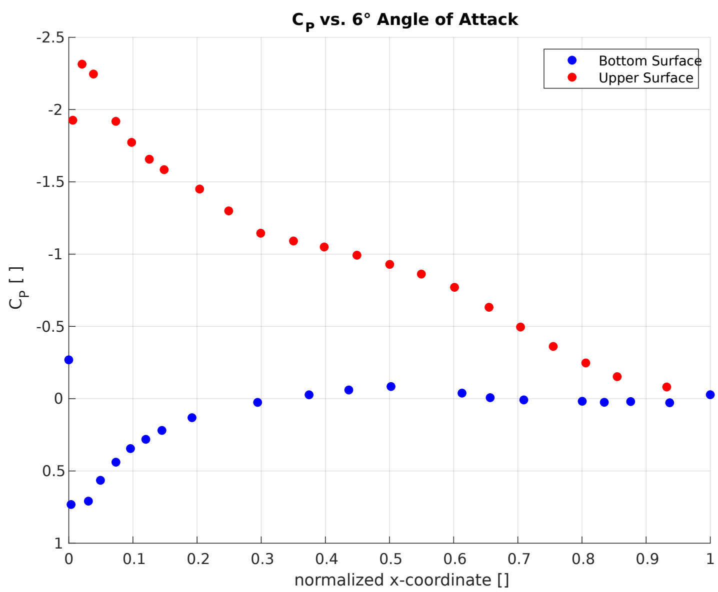

Figure 3.5: *Plot of the C_P in relationship to the normalized x component at a AoA of* $6°$.

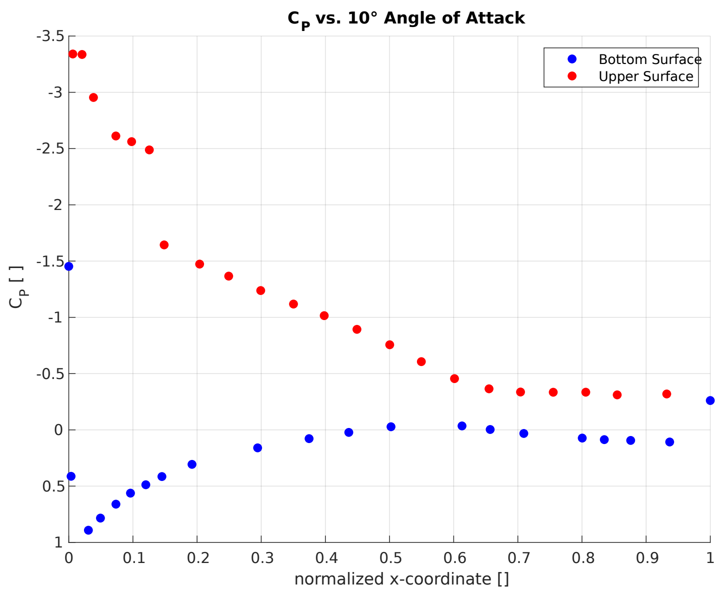

Figure 3.6: *Plot of the C_P in relationship to the normalized x component at a AoA of* $10°$.

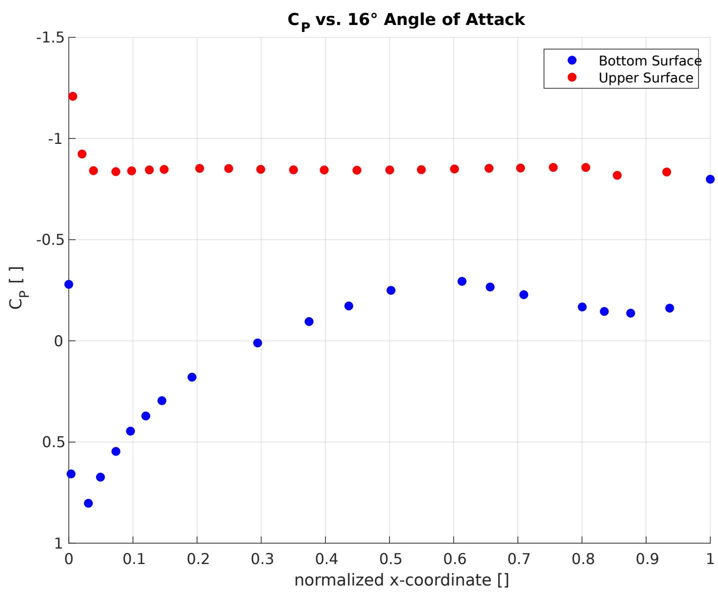

Figure 3.7: *Plot of the C_P in relationship to the normalized x component at a AoA of* $16°$.

Using Equation 3.1 and the following parameters, we find the Reynold's number shown below.

$$Re = \frac{\rho V L}{\mu} \tag{3.1}$$

$\rho = 1.225\,\mathrm{kg/m^3}$
$\mu = 18.18 \times 10^{-6}\,\mathrm{Pa\,s}$
$L = 0.101\,\mathrm{m}$
$V = 19.4\,\mathrm{m/s}$
$Re = 1.3203 \times 10^5$

4 Discussion

Figure 3.1 shows the coefficient of lift at angles of attack of $-4°$ to $16°$. The max C_l is around an AoA of $12°$, which is the stall angle. Figure 3.2 shows the lowest coefficient of drag is between $4°$ to $6°$. The C_d increases substantially after an AoA of $12°$ which further shows that is the stall angle. The aerodynamic moment is negative for all angles of attack tested and decreases as the angle of attack increases (see Figure 3.3). The moment in the pitch-down direction increases as the airfoil AoA increases.

In Figure 3.4, similar values of C_P are seen on the upper and lower surface of the airfoil. The AoA of $-4°$ is close to the zero-lift angle of attack as shown in Figure 3.1. The upper surface has a positive C_P near the leading edge, while the lower surface has a negative C_P resulting in a negative lift force.

Figure 3.5 shows that at an AoA of $6°$, the C_P increases steadily from the leading to trailing edge. There is no flow separation over the airfoil. In contrast, Figure 3.6 shows that when the angle of attack nears $10°$, the C_P levels off at a normalized x coordinate of 0.6 and the flow starts to separate. In Figure 3.7, the C_P is almost completely constant along the upper surface showing the flow is completely separated at an AoA of $16°$.

The stagnation point is where fluid contacting the airfoil has a velocity of zero. At this point, the coefficient of pressure, C_P, would be 1, *i.e.*, the pressure is equal to the total static pressure. From our data, at low angles of attack—*e.g.*, $-4°$ to $6°$—the C_P closest to 1 appears at the normalized x coordinate of zero (see Figure A.1). However, at angles of attack greater than $6°$, the C_P closest to 1 moves to the right on the lower surface of the airfoil with a normalized x-coordinate of approximately 0.05 (see Figure A.3).

The motor frequency was set to 15 Hz for all angles of attack. Using calculations from Lab 2, the fluid velocity is around 19.4 m/s. The Reynolds number at this velocity is approximately 1.3203×10^5.

5

Conclusion

Using the Scanivalve DSA 3217 pressure transducers, we measured pressure from 43 taps on the upper and lower surfaces of an airfoil for a range of angle of attacks at a constant fluid velocity in the wind tunnel. We calculated the C_P, C_l, C_d, C_m from the Scanivalve data. The C_P graphs show flow separation from the upper surface of the airfoil as the angle of attack increases. This separation causes a stall which is seen by the sudden increase of the C_d in Figure 3.2, the maximum C_l in Figure 3.1, and the minimum C_m in Figure 3.3 at the stall angle. Also from the C_P graphs, the stagnation point can be seen moving away from the leading edge along the lower surface of the airfoil as the angle of attack increases.

Bibliography

Hu, Hui (2024). *Determination of the Aerodynamic Performance of a Low-Speed Airfoil based on Pressure Distribution Measurements*. Iowa State University. URL: `https://www.aere.iastate.edu/~huhui/teaching/2024-01S/AerE344/lab-instruction/AerE344L-Lab-05-instruction.pdf`.

A

Appendix A

A.1 Additional Figures

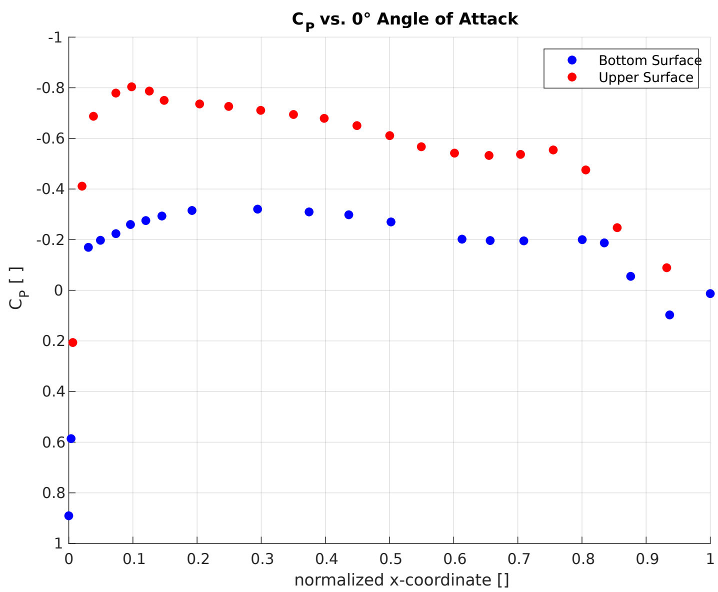

Figure A.1: *Plot of the C_P in relationship to the normalized x component at a AoA of* 0°.

A.2 Lab Apparatus Pictures

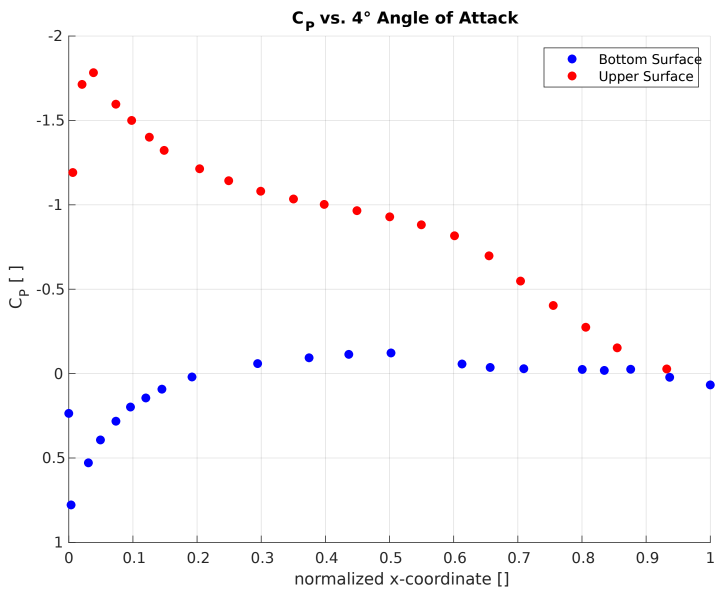

Figure A.2: *Plot of the C_P in relationship to the normalized x component at a AoA of 4°*

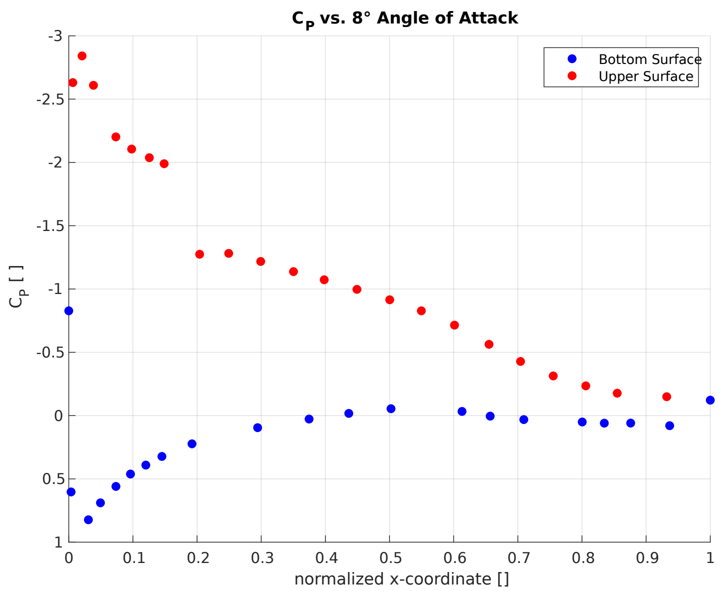

Figure A.3: *Plot of the C_P in relationship to the normalized x component at a AoA of 8°*

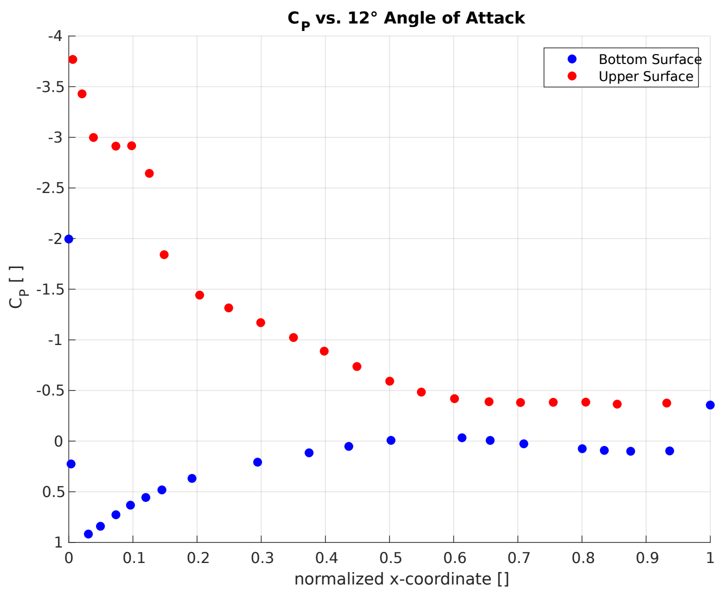

Figure A.4: *Plot of the C_P in relationship to the normalized x component at a AoA of* 12°

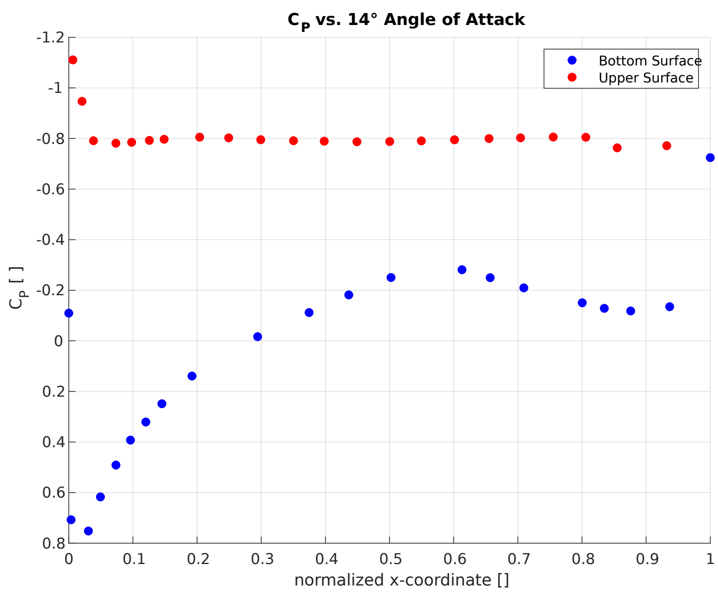

Figure A.5: *Plot of the C_P in relationship to the normalized x component at a AoA of* 14°

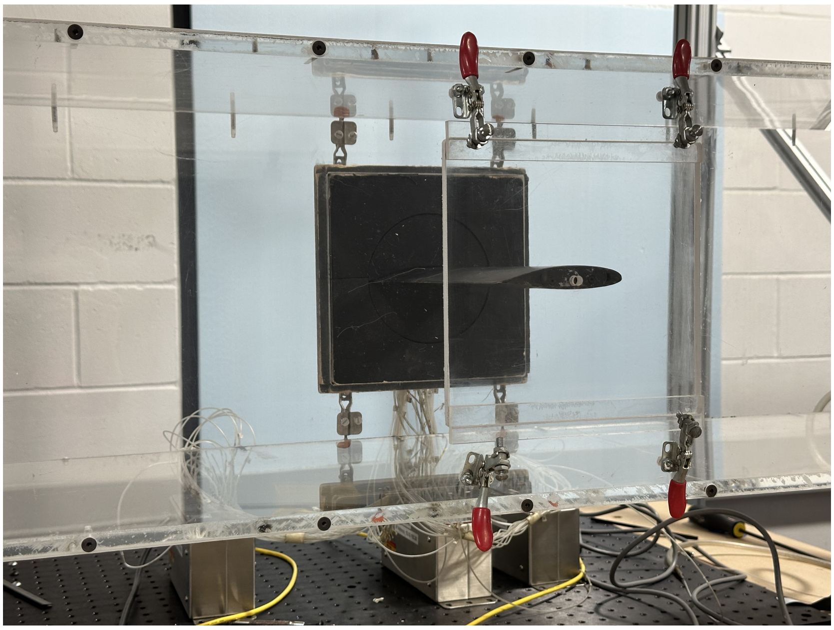

Figure A.6: *Image of Airfoil in Test Section.*

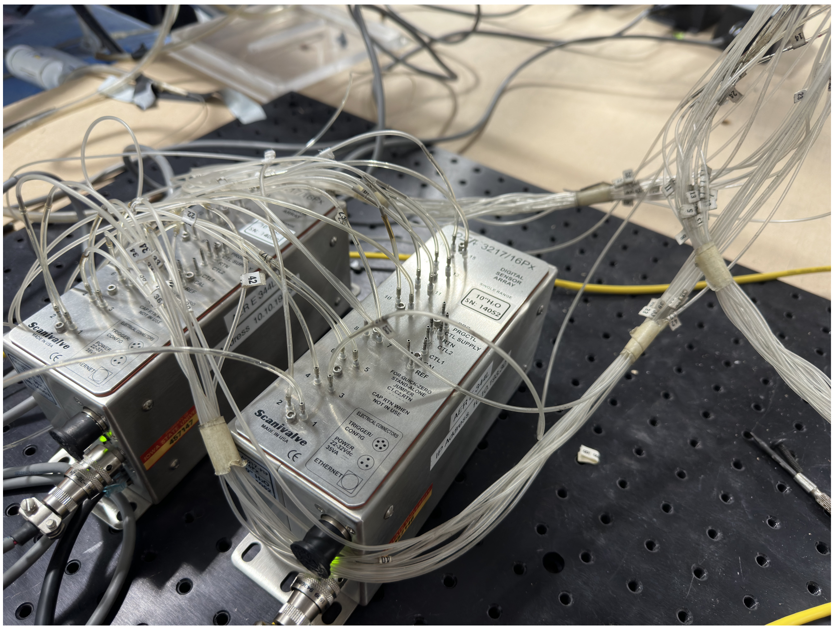

Figure A.7: *Image of the Scanivalve tester next to the test section.*

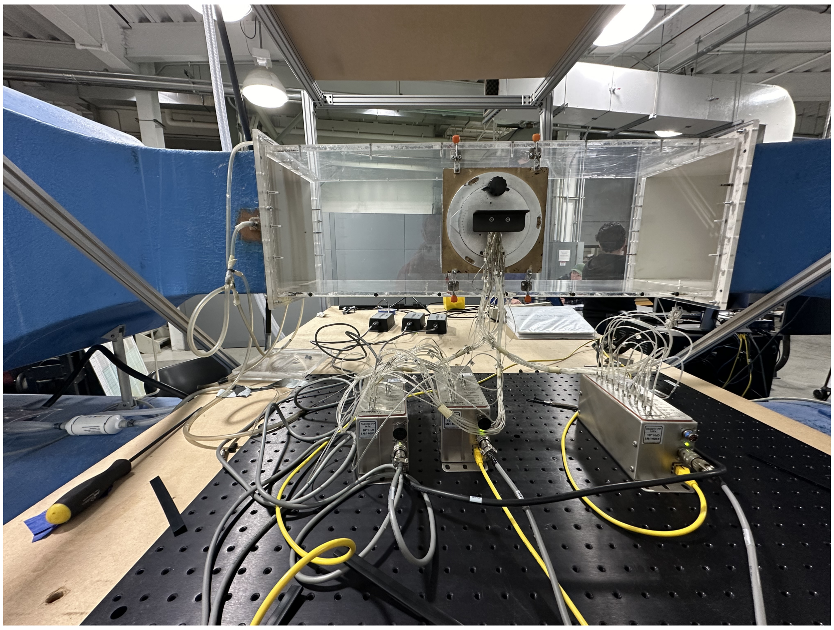

Figure A.8: *Image of the Scanivalve tester next to the test section.*

B

Appendix B

B.1 Data

Table B.1: *Coefficient of Pressure, C_P, at lower surface pressure taps (1-21) around the airfoil at different angles of attack.*

Tap	$-4°$	$0°$	$4°$	$6°$	$8°$	$10°$	$12°$	$14°$	$16°$
1	0.854	0.891	0.236	−0.269	−0.828	−1.453	−1.996	−0.109	−0.279
2	−0.104	0.586	0.778	0.732	0.603	0.413	0.225	0.707	0.657
3	−1.024	−0.170	0.529	0.709	0.823	0.892	0.918	0.752	0.803
4	−0.879	−0.198	0.393	0.565	0.689	0.784	0.841	0.617	0.673
5	−0.780	−0.224	0.282	0.439	0.560	0.660	0.727	0.491	0.546
6	−0.738	−0.260	0.198	0.345	0.462	0.562	0.633	0.392	0.446
7	−0.705	−0.275	0.144	0.281	0.391	0.488	0.557	0.321	0.371
8	−0.679	−0.293	0.092	0.220	0.323	0.415	0.482	0.249	0.296
9	−0.640	−0.315	0.020	0.132	0.223	0.307	0.368	0.139	0.180
10	−0.565	−0.321	−0.059	0.026	0.095	0.160	0.208	−0.017	0.010
11	−0.512	−0.310	−0.094	−0.027	0.027	0.078	0.115	−0.112	−0.095
12	−0.473	−0.298	−0.114	−0.060	−0.017	0.023	0.052	−0.182	−0.172
13	−0.427	−0.270	−0.122	−0.084	−0.054	−0.028	−0.007	−0.250	−0.249
14	−0.384	−0.202	−0.057	−0.038	−0.033	−0.035	−0.033	−0.281	−0.294
15	−0.387	−0.196	−0.036	−0.007	0.004	−0.003	−0.007	−0.250	−0.266
16	−0.304	−0.195	−0.029	0.009	0.032	0.032	0.026	−0.209	−0.228
17	0.053	−0.200	−0.025	0.018	0.051	0.073	0.075	−0.150	−0.167
18	0.094	−0.187	−0.019	0.025	0.060	0.087	0.092	−0.129	−0.145
19	0.116	−0.055	−0.026	0.020	0.059	0.094	0.100	−0.118	−0.137
20	0.126	0.097	0.022	0.028	0.080	0.108	0.097	−0.135	−0.162
21	−0.087	0.013	0.067	−0.027	−0.122	−0.261	−0.356	−0.724	−0.799

Table B.2: *Coefficient of Pressure, C_P, at upper surface pressure taps (22-43) around the airfoil at different angles of attack.*

Tap	$-4°$	$0°$	$4°$	$6°$	$8°$	$10°$	$12°$	$14°$	$16°$
22	−0.286	−0.089	−0.028	−0.081	−0.149	−0.319	−0.376	−0.772	−0.834
23	−0.348	−0.247	−0.153	−0.152	−0.177	−0.311	−0.365	−0.763	−0.818
24	−0.368	−0.475	−0.275	−0.247	−0.235	−0.335	−0.385	−0.805	−0.857
25	−0.356	−0.554	−0.404	−0.361	−0.313	−0.334	−0.383	−0.806	−0.857
26	−0.353	−0.537	−0.548	−0.496	−0.428	−0.336	−0.381	−0.803	−0.854
27	−0.359	−0.533	−0.698	−0.632	−0.563	−0.365	−0.389	−0.800	−0.853
28	−0.380	−0.542	−0.817	−0.770	−0.714	−0.455	−0.419	−0.795	−0.849
29	−0.428	−0.567	−0.882	−0.862	−0.828	−0.606	−0.484	−0.791	−0.846
30	−0.465	−0.611	−0.929	−0.929	−0.915	−0.756	−0.592	−0.788	−0.844
31	−0.480	−0.650	−0.965	−0.992	−0.997	−0.893	−0.737	−0.787	−0.843
32	−0.480	−0.679	−1.002	−1.049	−1.073	−1.015	−0.888	−0.789	−0.844
33	−0.467	−0.694	−1.035	−1.091	−1.137	−1.118	−1.023	−0.791	−0.845
34	−0.451	−0.711	−1.081	−1.145	−1.218	−1.238	−1.170	−0.795	−0.847
35	−0.429	−0.726	−1.143	−1.299	−1.281	−1.366	−1.315	−0.803	−0.852
36	−0.396	−0.736	−1.214	−1.450	−1.275	−1.473	−1.442	−0.805	−0.852
37	−0.340	−0.750	−1.323	−1.584	−1.990	−1.644	−1.841	−0.797	−0.847
38	−0.337	−0.787	−1.401	−1.656	−2.037	−2.488	−2.644	−0.792	−0.845
39	−0.294	−0.804	−1.500	−1.773	−2.106	−2.562	−2.917	−0.785	−0.840
40	−0.197	−0.779	−1.596	−1.919	−2.202	−2.612	−2.913	−0.781	−0.836
41	0.043	−0.687	−1.783	−2.246	−2.609	−2.954	−2.998	−0.791	−0.841
42	0.368	−0.411	−1.714	−2.314	−2.841	−3.336	−3.429	−0.947	−0.923
43	0.821	0.206	−1.191	−1.926	−2.630	−3.341	−3.769	−1.111	−1.208

Table B.3: *C_d, C_l, and C_m at different airfoil angles of attack.*

	−4°	0°	4°	6°	8°	10°	12°	14°	16°
C_d	0.035	0.017	−0.010	−0.011	−0.004	0.003	0.028	0.219	0.260
C_P	−0.038	0.339	0.838	0.988	1.099	1.175	1.211	0.706	0.754
C_m	−0.064	−0.141	−0.267	−0.297	−0.320	−0.331	−0.336	−0.303	−0.326

C

Appendix C

C.1 Lab5Analysis.m

```
clear; clc; close all;

figure_dir = "../Figures/";

%% port Cordinates

coords = [0.0000, 0.0036, 0.0306, 0.0494, 0.0735, 0.0962, 0.1201, ...
    0.1452, 0.1921, 0.2944, 0.3746, 0.4365, 0.5023, 0.6130, 0.6569, ...
    0.7093, 0.8004, 0.8348, 0.8759, 0.9367, 1.0000 0.9321, 0.8549, ...
    0.8059, 0.7552, 0.7042, 0.6551, 0.6013, 0.5496, 0.5003, 0.4492, ...
    0.3982, 0.3503, 0.2992, 0.2493, 0.2040, 0.1487, 0.1256, 0.0980, ...
    0.0734, 0.0385, 0.0207, 0.0063, 0; ...
    0.0000, -0.0126, -0.0293, -0.0355, -0.0418, -0.0462, -0.0502, ...
    -0.0539, -0.0585, -0.0641, -0.0653, -0.0640, -0.0609, -0.0486, ...
    -0.0415, -0.0322, -0.0158, -0.0105, -0.0056, -0.0023, 0.0000, ...
    0.0177, 0.0386, 0.0514, 0.0639, 0.0755, 0.0851, 0.0935, 0.0992, ...
    0.1027, 0.1045, 0.1047, 0.1036, 0.1015, 0.0979, 0.0930, 0.0838, ...
    0.0792, 0.0725, 0.0651, 0.0503, 0.0383, 0.0227,0];

coordsplot = [0.0000, 0.0036, 0.0306, 0.0494, 0.0735, 0.0962, 0.1201, ...
    0.1452, 0.1921, 0.2944, 0.3746, 0.4365, 0.5023, 0.6130, 0.6569, ...
    0.7093, 0.8004, 0.8348, 0.8759, 0.9367, 1.0000 0.9321, 0.8549, ...
    0.8059, 0.7552, 0.7042, 0.6551, 0.6013, 0.5496, 0.5003, 0.4492, ...
    0.3982, 0.3503, 0.2992, 0.2493, 0.2040, 0.1487, 0.1256, 0.0980, ...
    0.0734, 0.0385, 0.0207, 0.0063; ...
    0.0000, -0.0126, -0.0293, -0.0355, -0.0418, -0.0462, -0.0502, ...
    -0.0539, -0.0585, -0.0641, -0.0653, -0.0640, -0.0609, -0.0486, ...
    -0.0415, -0.0322, -0.0158, -0.0105, -0.0056, -0.0023, 0.0000, ...
    0.0177, 0.0386, 0.0514, 0.0639, 0.0755, 0.0851, 0.0935, 0.0992, ...
    0.1027, 0.1045, 0.1047, 0.1036, 0.1015, 0.0979, 0.0930, 0.0838, ...
    0.0792, 0.0725, 0.0651, 0.0503, 0.0383, 0.0227];

%% Average upload
deg4N = readtable('-4dg_updated - -4dg (1).csv','Range',"B1:AR1");
```

```
deg0 = readtable("0dg_updated - 0dg.csv",'Range',"B1:AR1");
deg4 = readtable("4dg_updated - 4dg.csv",'Range',"B1:AR1");
deg6 = readtable("6dg_updated - 6dg.csv",'Range',"B1:AR1");
deg8 = readtable("8dg_updated  - 8dg.csv",'Range',"B1:AR1");
deg10 = readtable("10dg_updated  - 10dg.csv",'Range',"B1:AR1");
deg12 = readtable("12dg_updated - 12dg.csv",'Range',"B1:AR1");
deg14 = readtable("14dg_updated - 14dg.csv",'Range',"B1:AR1");
deg16 = readtable("16dg_updated - 16dg.csv",'Range',"B1:AR1");

Average = [deg4N;deg0;deg4;deg6;deg8;deg10;deg12;deg14;deg16];

FirstC = Average(:,1);
FirstC.Properties.VariableNames{1} = 'FirstC_Var1';

Averagedata = [Average,FirstC];

deg4NAE = readmatrix('-4dg_updated - -4dg (1).csv','Range',"AS1:AT1");
deg0AE = readmatrix("0dg_updated - 0dg.csv",'Range',"AS1:AT1");
deg4AE = readmatrix("4dg_updated - 4dg.csv",'Range',"AS1:AT1");
deg6AE = readmatrix("6dg_updated - 6dg.csv",'Range',"AS1:AT1");
deg8AE = readmatrix("8dg_updated  - 8dg.csv",'Range',"AS1:AT1");
deg10AE = readmatrix("10dg_updated  - 10dg.csv",'Range',"AS1:AT1");
deg12AE = readmatrix("12dg_updated - 12dg.csv",'Range',"AS1:AT1");
deg14AE = readmatrix("14dg_updated - 14dg.csv",'Range',"AS1:AT1");
deg16AE = readmatrix("16dg_updated - 16dg.csv",'Range',"AS1:AT1");

AverageAE = [deg4NAE;deg0AE;deg4AE;deg6AE;deg8AE;...
    deg10AE;deg12AE;deg14AE;deg16AE];

%% Finding average pressure for each Pannel
for i=1:43
    j = i+1;
    % Extract the variables for addition
    var_i = Averagedata.(Averagedata.Properties.VariableNames{i});
    var_j = Averagedata.(Averagedata.Properties.VariableNames{j});

    % Calculate average and store in result matrix
    average_pressure(:, i) = (var_i + var_j) / 2;
end

for i=1:43
    j = i+1;
    % Extract the variables for addition
    % Calculate average and store in result matrix
    middle_coord(:, i) = (coords(:,j) - coords(:,i));
    half_coord(:,i) = 0.5*(coords(:,j) + coords(:,i));
end

for i = 1:9
    delN(i,:) = average_pressure(i,:).*middle_coord(1,:);
    delA(i,:) = -average_pressure(i,:).*middle_coord(2,:);
```

```
    delM(i,:) = (-(average_pressure(i,:).*middle_coord(1,:)) ...
        .*half_coord(1,:)-(average_pressure(i,:).*middle_coord(2,:)) ...
        .*half_coord(2,:));
end

NSum = sum(delN,2);
ASum = sum(delA,2);
MSum = sum(delM,2);

AOA = [-4;0;4;6;8;10;12;14;16];

for i = 1:9
    Lift_per_unit(i,:) = NSum(i,:).*cosd(AOA(i,:))...
        -ASum(i,:).*sind(AOA(i,:));
    Drag_per_unit(i,:) = NSum(i,:).*sind(AOA(i,:))...
        +ASum(i,:).*cosd(AOA(i,:));
    q(i,:) = 1.1.*(AverageAE(i,1) - AverageAE(i,2));
end

C_l = Lift_per_unit./q;
C_d = Drag_per_unit./q;
C_m = MSum./q;

Averagedata_pressure = Average;

for i=1:9
    C_p_table(i,:) = (Averagedata_pressure(i,:) - AverageAE(i,2))./q(i,:);
    C_p = table2array(C_p_table);
end

%% Graphs
figure
plot(AOA,C_l,"k","LineWidth",2)
title_str = "C_L vs. Angle of Attack";
title(title_str)
xlabel("AoA [°]")
ylabel("C_L [ ]")
grid on
saveas(gcf, figure_dir + title_str + ".svg");

figure
plot(AOA,C_d,"k","LineWidth",2)
title_str = "C_D vs. Angle of Attack";
title(title_str)
xlabel("AoA [°]")
ylabel("C_D [ ]")
grid on
saveas(gcf, figure_dir + title_str + ".svg");

figure
plot(AOA,C_m,"k","LineWidth",2)
```

```
title_str = "C_M vs. Angle of Attack";
title(title_str)
xlabel("AoA [°]")
ylabel("C_M [ ]")
grid on
saveas(gcf, figure_dir + title_str + ".svg");

figure
hold on
scatter(coordsplot(1,(1:21)),(C_p(1,1:21)),"Blue","filled")
scatter(coordsplot(1,(22:43)),(C_p(1,22:43)),"Red","filled")
hold off
set (gca,'YDir','reverse')
title_str = "C_p vs. -4° Angle of Attack";
title(title_str)
xlabel("normalized x-coordinate []")
ylabel("C_P [ ]")
grid on
legend("Bottom Surface","Upper Surface")
saveas(gcf, figure_dir + title_str + ".svg");

figure
hold on
scatter(coordsplot(1,(1:21)),(C_p(2,1:21)),"Blue","filled")
scatter(coordsplot(1,(22:43)),(C_p(2,22:43)),"Red","filled")
hold off
set (gca,'YDir','reverse')
title_str = "C_P vs. 0° Angle of Attack";
title(title_str)
xlabel("normalized x-coordinate []")
ylabel("C_P [ ]")
grid on
legend("Bottom Surface","Upper Surface")
saveas(gcf, figure_dir + title_str + ".svg");

figure
hold on
scatter(coordsplot(1,(1:21)),(C_p(3,1:21)),"Blue","filled")
scatter(coordsplot(1,(22:43)),(C_p(3,22:43)),"Red","filled")
hold off
set (gca,'YDir','reverse')
title_str = "C_P vs. 4° Angle of Attack";
title(title_str)
xlabel("normalized x-coordinate []")
ylabel("C_P [ ]")
grid on
legend("Bottom Surface","Upper Surface")
saveas(gcf, figure_dir + title_str + ".svg");

figure
hold on
```

```
scatter(coordsplot(1,(1:21)),(C_p(4,1:21)),"Blue","filled")
scatter(coordsplot(1,(22:43)),(C_p(4,22:43)),"Red","filled")
hold off
set (gca,'YDir','reverse')
title_str = "C_P vs. 6° Angle of Attack";
title(title_str)
xlabel("normalized x-coordinate []")
ylabel("C_P [ ]")
grid on
legend("Bottom Surface","Upper Surface")
saveas(gcf, figure_dir + title_str + ".svg");

figure
hold on
scatter(coordsplot(1,(1:21)),(C_p(5,1:21)),"Blue","filled")
scatter(coordsplot(1,(22:43)),(C_p(5,22:43)),"Red","filled")
hold off
set (gca,'YDir','reverse')
title_str = "C_P vs. 8° Angle of Attack";
title(title_str)
xlabel("normalized x-coordinate []")
ylabel("C_P [ ]")
grid on
legend("Bottom Surface","Upper Surface")
saveas(gcf, figure_dir + title_str + ".svg");

figure
hold on
scatter(coordsplot(1,(1:21)),(C_p(6,1:21)),"Blue","filled")
scatter(coordsplot(1,(22:43)),(C_p(6,22:43)),"Red","filled")
hold off
set (gca,'YDir','reverse')
title_str = "C_P vs. 10° Angle of Attack";
title(title_str)
xlabel("normalized x-coordinate []")
ylabel("C_P [ ]")
grid on
legend("Bottom Surface","Upper Surface")
saveas(gcf, figure_dir + title_str + ".svg");

figure
hold on
scatter(coordsplot(1,(1:21)),(C_p(7,1:21)),"Blue","filled")
scatter(coordsplot(1,(22:43)),(C_p(7,22:43)),"Red","filled")
hold off
set (gca,'YDir','reverse')
title_str = "C_P vs. 12° Angle of Attack";
title(title_str)
xlabel("normalized x-coordinate []")
ylabel("C_P [ ]")
grid on
```

```
legend("Bottom Surface","Upper Surface")
saveas(gcf, figure_dir + title_str + ".svg");

figure
hold on
scatter(coordsplot(1,(1:21)),(C_p(8,1:21)),"Blue","filled")
scatter(coordsplot(1,(22:43)),(C_p(8,22:43)),"Red","filled")
hold off
set (gca,'YDir','reverse')
title_str = "C_P vs. 14° Angle of Attack";
title(title_str)
xlabel("normalized x-coordinate []")
ylabel("C_P [ ]")
grid on
legend("Bottom Surface","Upper Surface")
saveas(gcf, figure_dir + title_str + ".svg");

figure
hold on
scatter(coordsplot(1,(1:21)),(C_p(9,1:21)),"Blue","filled")
scatter(coordsplot(1,(22:43)),(C_p(9,22:43)),"Red","filled")
hold off
set (gca,'YDir','reverse')
title_str = "C_P vs. 16° Angle of Attack";
title(title_str)
xlabel("normalized x-coordinate []")
ylabel("C_P [ ]")
grid on
legend("Bottom Surface","Upper Surface")
saveas(gcf, figure_dir + title_str + ".svg");
```